Agricultural Water Management 224 (2019) 105744

Contents lists available at ScienceDirect

Agricultural Water Management

journal homepage: www.elsevier.com/locate/agwat

Water-scarcity footprints and water productivities indicate unsustainable wheat production in China

Jing Huang[a,b,*], Bradley G. Ridoutt[c,d], Kelly R. Thorp[e], Xuechun Wang[a], Kang Lan[a], Jun Liao[f], Xu Tao[g], Caiyan Wu[f], Jianliang Huang[g], Fu Chen[h,**], Laura Scherer[b]

[a] College of Life Science and Engineering, Southwest University of Science and Technology (SWUST), Mianyang, 621010, China
[b] Institute of Environmental Sciences (CML), Leiden University, 2333 CC, Leiden, the Netherlands
[c] Agriculture and Food, CSIRO, Clayton South, Melbourne, Victoria, 3169, Australia
[d] Department of Agricultural Economics, University of the Free State, Bloemfontein, 9300, South Africa
[e] USDA-ARS, U.S. Arid Land Agricultural Research Center, Maricopa, AZ, 85138, USA
[f] College of Environment and Resources, Southwest University of Science and Technology (SWUST), Mianyang, 621010, China
[g] College of Plant Science and Technology, Huazhong Agricultural University (HZAU), Wuhan, 430070, China
[h] College of Agronomy, China Agricultural University (CAU), Beijing, 100193, China

ARTICLE INFO

Keywords:
Food production
Environmental impacts
Water security
Hotspots
Crop distribution

ABSTRACT

Water shortage is a critical constraint limiting China's capacity for food security. To provide evidence supporting environmentally sustainable water use in food production, this study compared irrigation water productivities (IWPs) and water-scarcity footprints (WSFs) for China's wheat production at high spatial resolution. Contrary to previous water productivity studies assessing crop yield over total water consumption, it was found that IWPs in China's water-scarce northern regions were much lower than those in water-rich southern regions. The WSFs further demonstrated the larger environmental impacts resulting from irrigation in water-scarce northern regions. Hotspot regions, having IWPs in the lowest tercile ($< 5.2\,kg\,m^{-3}$) and WSFs in the highest tercile ($> 0.058\,m^3\,H_2O_e\,kg^{-1}$), were mainly located in the Huang-Huai-Hai and northwestern regions and accounted for 34% of the cropping area but 61% of irrigation water use. Historically, the south was also an important contributor of China's wheat production, but progressive shifts toward highly resource-efficient cropping in the Huang-Huai-Hai region has occurred. The paradox is that gains in total crop water efficiency have led to increased irrigation demand and water scarcity. Today, croplands suitable for wheat production lie fallow in some southern regions in the winter. A national reassessment of this situation is urgently needed.

1. Introduction

Feeding a growing population while minimizing global environmental impacts are twin challenges faced by the global food system (Davis et al., 2017; Foley et al., 2011; Scherer et al., 2018). As the world's most populous and largest food-consuming country, China's food security has been an issue of broad concern for a long time (Brown, 1997; Dalin et al., 2015; Heilig et al., 2009). Water shortage is recognized as the most critical constraint that limits China's capacity for food security (Du et al., 2014; Huang and Li, 2010; Khan et al., 2009). Although China's water resources are large in absolute terms, the average water resources per capita are less than one-third of the global average (Kang et al., 2017). Moreover, increasing demand, worsening water pollution, spatially and seasonally uneven water distributions, and climate change have aggravated the water shortage and deteriorated China's aquatic ecosystem (Cai et al., 2017; Xiong et al., 2009; Zuo et al., 2018).

The agricultural sector is responsible for the most water use in China, accounting for 63% (NBSC, 2011–2016NBSC, 2016NBSC, 2011–2016). To address the water for food dilemma in China, improving crop water productivity (WP), especially irrigation water productivity (IWP), has been an important measure for ensuring China's water and food security. IWP refers to the total crop yield divided by the total amount of irrigation water used for crops, i.e. it is high if crop yields are high and irrigation is low. China's national grain IWP has increased from $0.8\,kg\,m^{-3}$ in the early 1990s to $1.6\,kg\,m^{-3}$ in 2013 (Kang et al., 2017). Currently, improving WP and IWP remains the chief concern for China's agricultural water management (Du et al., 2015;

* Corresponding author at: College of Life Science and Engineering, Southwest University of Science and Technology (SWUST), Mianyang, 621010, China.
** Corresponding author at: College of Agronomy, China Agricultural University (CAU), Beijing, 100193, China.
E-mail addresses: huang.jing@swust.edu.cn (J. Huang), chenfu@cau.edu.cn (F. Chen).

https://doi.org/10.1016/j.agwat.2019.105744
Received 4 April 2019; Received in revised form 6 August 2019; Accepted 7 August 2019
Available online 20 August 2019

Geng et al., 2019; Kang et al., 2017). However, the WP (or IWP) concept has limited meaning when comparing the values from locations with different water scarcity backgrounds. This is because producing a crop with a high WP (or IWP) in a water-scarce region can cause more serious environmental impacts than producing a crop with a low WP in a water-rich region, as described by a life cycle assessment (LCA) based water-scarcity footprint (WSF) indicator (Ridoutt and Pfister, 2010a). Thus, the WP concept as well as other volumetric water-use indicators such as virtual water (VW), which for crops refers to the actual evapotranspiration over the crop yield (Chapagain and Hoekstra, 2008), or the VW-derived water footprint (WF_{vw}) (Aldaya et al., 2012), have the potential to misinform water management decisions (Ridoutt and Huang, 2012; Ridoutt and Pfister, 2010a).

It is reported that most global freshwater withdrawals currently occur in watersheds with extreme water stress (Ridoutt and Pfister, 2010b). That said, the urgent need to reduce the pressure that humanity exerts on the freshwater system does not arise from an absolute shortage of freshwater in the world but rather from the current pattern of freshwater use. Similar situations exist in the current state of crop production in China. For example, it is well-known that the extremely water-scarce North China Plain, with a water availability of less than 150 m^3 per capita per year, produces more than half of the national wheat and one-third of maize (CMWR, 2000–2015CMWR, 2015CMWR, 2000–2015; NBSC, 2011–2016NBSC, 2016NBSC, 2011–2016). The growing demand for irrigation water in this region has resulted in an overdraft of groundwater and therefore falling groundwater tables and increased land degradation. A number of studies have focused on this issue and mitigation strategies have been identified, such as improving the WP (or IWP) of crop production from a technological perspective and restricting the amount of water extraction from a policy perspective (Dalin et al., 2015; Kang et al., 2017; Yang et al., 2003). However, as mentioned above, these strategies focus on the local conservation of water rather than considering environmental impacts at the national scale, failing to provide useful information for supporting environmentally sustainable water use in China's food production.

To present a picture of national water use associated with wheat production and identify relevant hotspots, this study compared both the IWPs and WSFs of wheat production across China. A geospatial simulation tool (GeoSim) was applied to manage the FAO AquaCrop model for spatial simulations of wheat yield and irrigation water consumption from 2010 to 2015 (2015 being the most recent year for which most of the data were available). Hotspot regions with low IWPs but high WSFs were identified with a spatial resolution of 5 arc-minutes and were also presented at the scale of China's agro-ecological zones (AEZs). The overall goal was to provide scientific evidence that will enable policies to set national agricultural water use priorities across regions by considering the environmental implications of meeting food security.

2. Material and methods

2.1. Wheat yield and irrigation water consumption modeling

Wheat yields and irrigation water consumptions were modeled by the widely applied FAO AquaCrop model (version 6.1) (http://www.fao.org/aquacrop), which simulated attainable yield as a function of water consumption under rain-fed or irrigated conditions on a daily step (Raes et al., 2009; Steduto et al., 2009). To facilitate the use of AquaCrop and other models for a high number of spatial simulations, a model-independent and open-source tool named GeoSim was previously developed as a plug-in for Quantum GIS (QGIS, https://www.qgis.org) and its application has been improved to efficiently work at China's national scale (Huang et al., 2019; Thorp and Bronson, 2013). GeoSim automates batch simulations with AquaCrop for different locations by passing geospatial data from polygons in a base shapefile to the model input files, and then similarly passing model outputs back to the base shapefile (Thorp and Bronson, 2013).

Six types of input data were used for the simulations: 1) crop distribution; 2) climate data; 3) crop parameters; 4) soil parameters; 5) initial soil water conditions; and 6) management data. A shapefile (vector data) of national wheat distribution in 2015 was created from a raster dataset with a resolution of 5 arc-minutes (Appendix A., Fig. A.1). Daily climate data from 825 meteorological stations across China from 2010 to 2015 were obtained from the National Meteorological Information Center (NMIC, http://data.cma.cn). Crop parameters including sowing dates, sowing density, growing stages and harvest dates were also obtained from the NMIC. Additional crop data such as crop transpiration, yield formation, and soil water stresses were based on the conservative wheat parameters provided by the AquaCrop reference manual (http://www.fao.org/aquacrop) and studies which documented these parameters for both spring and winter wheat production modeling in China (Huang et al., 2019). Primary soil data applied to identify soil textures were obtained from the Harmonized World Soil Database (Wieder et al., 2014). The indicative values of several soil hydraulic parameters for each soil type were obtained from the AquaCrop reference manual. To avoid modeling failures caused by low soil water content that affects canopy development, the initial soil water contents were assumed to be at field capacity, which was the default value of AquaCrop. Due to the lack of detailed national irrigation management data, irrigation water consumption and wheat yields under irrigation conditions were modeled by applying the option of "Determination of Net Irrigation Requirement" in AquaCrop, which are calculated by adding a small amount of water to the soil profile each day when the root zone depletion exceeds a specified threshold. The threshold for the allowable root zone depletion was set as 50% of the readily available soil water, which was identified as a threshold for wheat irrigation management in China (Zhang et al., 2015). The default rain-fed condition in AquaCrop was applied to simulate the wheat yield under rain-fed conditions. Other management effects such as fertilizer application and ground surface cover were disregarded. Groundwater characteristics such as the depth and quality were not considered due to the lack of a detailed national dataset. All the input files of climate, crop, soil, initial condition and irrigation management were prepared according to the AquaCrop formats. Besides these files, the AquaCrop modeling requires day numbers to indicate the first and last days of cropping and simulation periods for each year: the calculation of these variables follows from our previous study (Huang et al., 2019).

After all the input files were prepared, GeoSim was used to pass only the names of the files and day numbers corresponding to each spatial unit in the base layer shapefile to AquaCrop's project file, which controls the AquaCrop simulations. By minimizing the spatial inputs and identifying unique response units—unique combinations of climate, crop, soil and day numbers, the efficiency of AquaCrop in conducting national-scale simulations was improved (Huang et al., 2019). As the model completed the simulation, the results for wheat yields and irrigation water consumptions under irrigated conditions and wheat yields under rain-fed conditions were post-processed by GeoSim and native QGIS tools. Finally, wheat yields and irrigation water consumptions from the base shapefile were converted back to raster datasets with a resolution of 5 arc-minutes. Further details on the post-processing is described in our previous study (Huang et al., 2019).

2.2. Irrigation water productivity calculation

Irrigation water productivity for wheat production in each grid cell (IWP_{grid}, kg m^{-3}) was defined as the total wheat production of each grid cell (P_{grid}, kg) divided by the total irrigation water consumption of each grid cell (I_{grid}, m^3):

$$IWP_{grid} = P_{grid}/I_{grid} \quad (1)$$

$$P_{grid} = (Y_{irri} \cdot F_{irri} + Y_{rain} \cdot (1 - F_{irri})) \cdot A \cdot 1000 \quad (2)$$

Fig. 1. China's first-order agro-ecological zones (AEZs). The number of the AEZs represents codes linked to their names (Liu and Chen, 2005). Each first-order AEZ includes several sub-order AEZs.

$$I_{grid} = I_{cons} \bullet F_{irri} \bullet A \bullet 10 \quad (3)$$

where Y_{irri} (t ha^{-1}) is the wheat yield under irrigated conditions; Y_{rain} (t ha^{-1}) is the wheat yield under rain-fed conditions; A (ha) is the area of wheat; I_{cons} (mm) is the amount of irrigation water consumption; F_{irri} is the fraction of irrigated cropland compared to the total cropland in each grid cell. The areas of the irrigated croplands and the total croplands at a county level were obtained for the year 2015 from national statistics (NBSC, 2011–2016NBSC, 2016NBSC, 2011–2016). This data was used to derive the F_{irri} for each county, which was subsequently converted to a raster dataset (Fig. A.2). We assumed that in each county, the irrigation water use was equally distributed among the area equipped for irrigation.

The IWPs of wheat production across China were presented in a raster map with a resolution of 5 arc-minutes. In addition, the grid-based IWPs were aggregated to average IWPs for each of China's agro-ecological zones (AEZs, Fig. 1) (Eq. (4)), which were defined based on climatic, soil and landform characteristics (Liu and Chen, 2005).

$$IWP_{AEZ} = \sum (IWP_{grid} \bullet I_{grid}) / \sum I_{grid} \quad (4)$$

2.3. Water-scarcity footprint calculation

The water-scarcity footprint in each grid cell (WSF_{grid}, m^3 H_2Oe kg^{-1}) was calculated by using a water scarcity index (WSI)—related to the ratio of water consumption to water availability—to express the environmental relevance of water use (Pfister et al., 2009):

$$WSF_{grid} = (I_{grid}/P_{grid}) \bullet WSI_{grid} \quad (5)$$

The gird-based WSIs were originated from a global dataset for the decade 2000–2009; then, the data were rescaled to the period of 2010–2015 by using the data of water availability, water use and precipitation for each of China's first-order basins (CMWR, 2000–2015CMWR, 2015CMWR, 2000–2015; Scherer and Pfister, 2016). The primary 30 arc-minute data were disaggregated by bilinear interpolation to 5 arc-minutes. The raster map of WSIs can be found in the Appendix A. (Fig. A.3).

The WSFs of wheat production across China were also presented in both a raster map with a resolution of 5 arc-minutes and a AEZ map. The WSFs for each of China's AEZs were calculated by the following equation:

$$WSF_{AEZ} = \sum (WSF_{grid} \bullet P_{grid}) / \sum P_{grid} \quad (6)$$

2.4. Hotspots identification

To identify the hotspot regions, IWPs and WSFs at both grid and AEZ scales were classified as low, moderate and high by dividing them into terciles, i.e. if they were below the 33.3% quantile (here IWP $<$ 5.2 kg m^{-3}; WSF $<$ 0.0065 m^3 H_2Oe kg^{-1}), between 33.3% and 66.7%, and above 66.7% (here IWP $>$ 15.8 kg m^{-3}; WSF $>$ 0.058 m^3 H_2Oe kg^{-1}). Thus, there can be nine combinations of IWPs and WSFs. The combinations were mapped using a matrix for color coding, and the corresponding wheat areas identified by each color were calculated and presented as percentages of the total wheat area. The hotspot regions were defined as the regions with low IWPs but high WSFs, which means a lot of irrigation water is used for wheat production in water scarce regions. Trade-offs can occur if IWP is low (i.e. water is wasted) but WSF is low (i.e. environmental impacts are low because of water abundance), or if IWP is high (i.e. water is saved) but WSF is also high (i.e. environmental impacts are high because of water scarcity). Since there was considerable uncertainty in the choice of boundaries, which would be further increased by combining two indicators with different units, we judged this qualitative representation as adequate for the type of information being analyzed rather than including more precise quantitative details.

3. Results

3.1. Wheat production and irrigation water consumption

The highest amounts of grid-based wheat production were mainly observed in the Huang-Huai-Hai AEZs (Fig. A.4a). The total production of these AEZs contributed to approximately 60% of the total national wheat production. Similarly, the highest amount of irrigation consumption for wheat production was also observed in the in the Huang-Huai-Hai AEZs (Fig. A.4b). Since the amount of precipitation is very low in most of the region during the winter wheat cropping season, irrigation is essential for wheat growth. It accounted for approximately 66% of the total national irrigation consumption for wheat production.

3.2. Irrigation water productivities and water-scarcity footprints

IWPs vary largely across regions, in line with differences in wheat yield and irrigation intensity. Most of the rain-fed or idly irrigated (unnecessarily irrigated without achieving any yield improvements) wheat production areas were located in the water-rich southern region (Fig. 2a). Low irrigation water consumption in some southern and northeastern regions resulted in much higher IWPs ($>$ 20.0 kg m^{-3}) compared to wheat grown in some northern, northwestern and southwestern regions ($<$ 2.5 kg m^{-3}). According to the AEZ scale (Fig. 2b), the Northwest AEZs had much lower IWPs ($<$ 2.5 kg m^{-3}), while some Southwest, Sichuan Basin and Northeast AEZs had much higher IWPs ($>$ 20.0 kg m^{-3}). If idle irrigation was avoided, most AEZs in the southern regions could have higher IWPs, e.g., the IWP of the Southwest AEZ encoded as 9.2 may increase from 31.3 to 35.6 kg m^{-3}.

Larger environmental impacts resulted from irrigation in water-

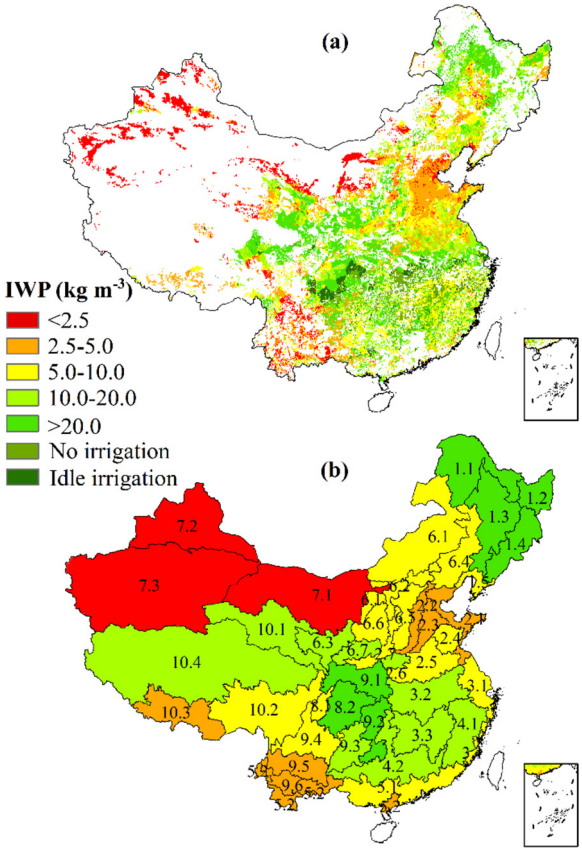

Fig. 2. Irrigation water productivities (IWP, kg m^{-3}) with a resolution of 5 arc-minutes (a) and (b) at the scale of agro-ecological zones (AEZs). White indicates no data or no wheat production. The number of the AEZs represents codes linked to their names (Liu and Chen, 2005). The integer part of the numbers indicates the code of first-order AEZs. For the names of the first-order AEZs, please refer to Fig. 1. Idle irrigation means the application of irrigation does not increase wheat yield compared with rain-fed wheat.

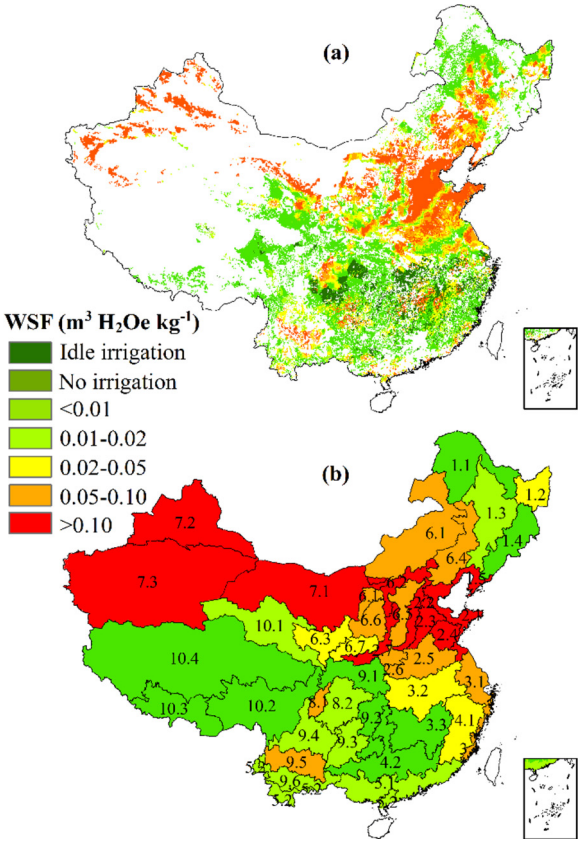

Fig. 3. Water-scarcity footprints (WSFs, m^3 H_2Oe kg^{-1}) with a resolution of 5 arc-minutes (a) and (b) at the scale of agro-ecological zones (AEZs). White indicates no data or no wheat production. The number of the AEZs represents codes linked to their names (Liu and Chen, 2005). The integer part of the numbers indicates the code of first-order AEZs. For the names of the first-order AEZs, please refer to Fig.1.

scarce regions, such as the Huang-Huai-Hai and northwestern regions (Fig. 3a). The WSFs of wheat in these regions were higher than 0.10 m^3 H_2Oe kg^{-1}. In contrast, the WSFs of wheat produced in some southern and northeastern regions were less than 0.01 m^3 H_2Oe kg^{-1}. At the AEZ scale (Fig. 3b), the Northwest AEZs as well as some Huang-Huai-Hai AEZs had much higher WSFs (> 0.10 m^3 H_2Oe kg^{-1}), while most Northeast AEZs and most AEZs in southern China had much lower WSFs (< 0.02 m^3 H_2Oe kg^{-1}).

3.3. Hotspot regions

The hotspot regions were identified as the grid cells with IWPs in the lowest tercile (< 5.2 kg m^{-3}) but with WSFs in the highest tercile (> 0.058 m^3 H_2Oe kg^{-1}) (marked red in Fig. 4a). The hotspot regions accounted for 34% of the total wheat cropping area (Fig. 4c), 32% of the national wheat production, and 61% of the national irrigation consumption for wheat production. Most hotspot regions were located in the Huang-Huai-Hai and northwestern regions. The most sustainable water use was found in the northeastern and southern regions, accounting for 11% of the national wheat cropping area (dark green in Fig. 4a). At the AEZ scale (Fig. 4b), the hotspot AEZs were identified as the Northwest and several Huang-Huai-Hai AEZs. Some AEZs in the Huang-Huai-Hai region and surroundings also had very high WSFs, but moderate IWPs (light coral in Fig. 4c).

4. Discussion

4.1. Comparison with other research

Most previous studies focus on the water productivity (WP) of wheat production (Cao et al., 2015; Huang and Li, 2010; Liu et al., 2007a, 2007b), the virtual water (VW) (Siebert and Döll, 2010; Sun et al., 2013) or the VW-derived water footprint (WF_{vw}) (Cao et al., 2014; Mekonnen and Hoekstra, 2010; Zhuo et al., 2016). To our knowledge, IWPs and WSFs for wheat production have not yet been estimated with such a high spatial resolution at the national scale. This impeded conducting a detailed spatial comparison with other research. To ease the comparison, the grid-based IWPs and WSFs were aggregated to national and regional average values and compared with literature values after harmonizing the concepts (e.g., WP vs IWP) and units (Table 1). The national and regional average IWPs in this study were higher than those derived from the literature (Cao et al., 2015; Huang and Li, 2010; Mekonnen and Hoekstra, 2010; Sun et al., 2013; Zhuo et al., 2016). An important reason is that most other studies used the wheat yield data from statistics or scaled the modeled yields to fit the statistics, but applied modeled water consumption values under full irrigation (Cao et al., 2015; Mekonnen and Hoekstra, 2010), which mixes optimal irrigation with suboptimal yields and may therefore overestimate the irrigation water consumption and result in lower IWPs. In contrast, by applying the option of “Determination of Net Irrigation Requirements” in AquaCrop without considering stress factors such as low fertility and high salinity, this study consistently assumes optimal conditions, but may overestimate the wheat yield and result in higher IWPs. The

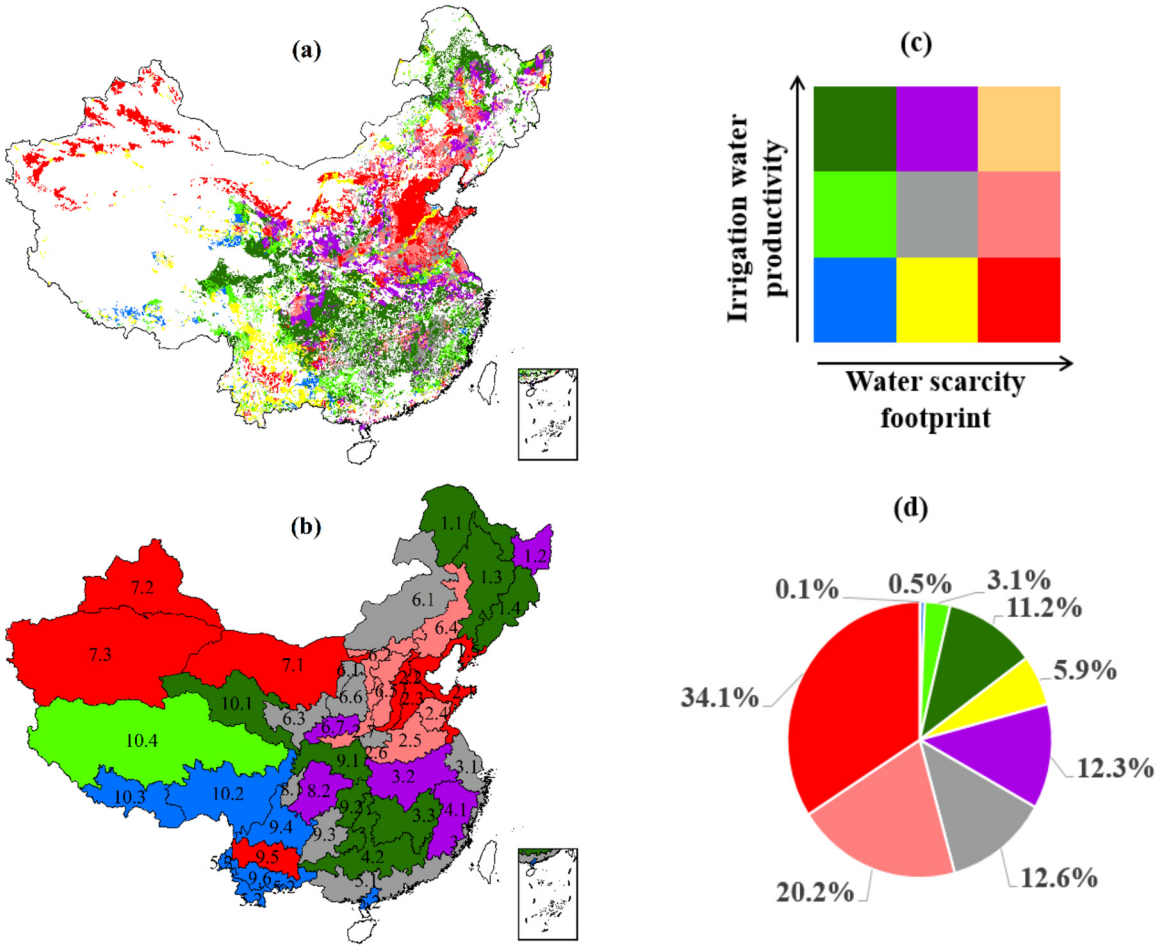

Fig. 4. Hotspot regions with a resolution of 5 arc-minutes (a) and (b) at the scale of agro-ecological zones (AEZs). Hotspots depend on IWPs and WSFs. Their synergies and trade-offs are depicted by a color matrix (c). The pie chart displays the share of each combination of IWPs and WSFs (d). White indicates no data or no wheat production. The number of the AEZs represents codes linked to their names (Liu and Chen, 2005). The integer part of the numbers indicates the code of first-order AEZs. For the names of the first-order AEZs, please refer to Fig. 1. (For interpretation of the references to colour in the text, the reader is referred to the web version of this article.).

Table 1
Comparison of the results with previous studies.

Item	Location	Reference	Studied year	Result	Note
IWP ($kg\ m^{-3}$)	China	This study	2010–2015	5.5	Irrigation-weighted IWP
		Cao et al. (2015)	1998–2010	3.9	Based on the WP and the ratio of blue water consumption
		Zhuo et al. (2016)	2008	3.2	Based on the VW-derived blue water footprint
		Mekonnen and Hoekstra (2010)	1996–2005	2.1	Based on the VW-derived blue water footprint
		Sun et al. (2013)	1979–2009	1.9	Based on the blue VW
	The northern regions	This study	2010–2015	3.5	For wheat produced in the Hai basin
		Huang and Li (2010)	1997–2004	1.8	Based on the WP and the ratio of blue water consumption for wheat produced in Hai basin
		Mekonnen and Hoekstra (2010)	1996–2005	1.9	For wheat produced in Yellow (Huang) basin
		Sun et al. (2013)	1979–2009	2.2	For wheat produced in Huang-Huai-Hai basins
	The southern regions	This study	2010–2015	14.4	For wheat produced in Yangtze basin
		Huang and Li (2010)	1997–2004	19.4	For wheat produced in Chang (Yangtze) basin
		Mekonnen and Hoekstra (2010)	1996–2005	5.8	For wheat produced in Yangtze basin
		Sun et al. (2013)	1979–2009	5.3	For wheat produced in the middle-lower reaches of Yangtze basin
WSF ($m^3\ H_2Oe\ kg^{-1}$)	China	This study	2010–2015	0.11	Production-weighted WSF
		Pfister and Bayer (2014)	2000	0.27	Production-weighted WSF based on WSI at the watershed level (1961–1990)
		Scherer and Pfister (2016)	2000	0.16	Based on country-specific WSI (2001–2010)

average national wheat yield (the total production divided by the total cropping area) in this study was 6.5 t ha^{-1}, while the average national data from the statistics during 2010–2015 was 5.0 t ha^{-1} (NBSC, 2011–2016NBSC, 2016NBSC, 2011–2016). Other reasons such as different studied time series and spatial resolutions may also result in higher IWPs in this study compared with previous studies. Higher wheat yields were also a reason for lower WSFs in this study compared with previous studies (Pfister and Bayer, 2014; Scherer and Pfister, 2016). In addition, this study calculated the national WSF as a production-weighted average based on gridded data for both water consumption and WSI, while Pfister and Bayer (2014) applied water consumption at the grid level but WSIs at the watershed level, and Scherer and Pfister (2016) focused their study on spatially explicit WSIs and only used national-scale crop production data to calculate WSFs for a few case studies. The different methods and different studied time series can also cause different results.

To identify the hotspot regions, the relative IWP and WSF values across China rather than the absolute values are more meaningful. Despite different absolute values among the studies, the spatial variation identified in IWPs and WSFs by this study resembles other studies (Huang and Li, 2010; Mekonnen and Hoekstra, 2010; Pfister and Bayer, 2014; Sun et al., 2013). The water-scarce northern regions such as the Huang, Huai, and Hai basins always had lower IWPs than the water-rich southern regions such as the Yangtze basin. For example, this study found that the IWP of wheat produced in the Hai basin was 3.5 kg m^{-3}, while that in the Yangtze basin was 14.4 kg m^{-3}. Similar results were obtained from Huang and Li (2010) who estimated an IWP of 1.8 kg m^{-3} for the Hai basin and an IWP of 19.4 kg m^{-3} for the Yangtze basin. Detailed regional WSF values were not available in previous studies, but the global map in Pfister and Bayer (2014) demonstrated a similar trend as this study, illustrating that the WSFs of the northern regions such as the Huang-Huai-Hai basins and northwest area were much higher than most southern regions.

4.2. Implications of this study

Previous studies have reported that wheat production in China's water-scarce northern regions (e.g., Huang-Huai-Hai basins) had higher WPs than most southern regions (e.g., Yangtze basin) (Cao et al., 2015; Huang and Li, 2010; Liu et al., 2007a). This WP indicator, which integrates green (i.e. soil moisture) and blue water (i.e. groundwater or surface water) into a single assessment of water consumption, is confusing, as the consumption of green water is not equivalent to the consumption of blue water. By assessing the blue water-related IWPs, this study presents data contrary to what was previously thought; IWPs in China's water-scarce northern regions (e.g., the Huang-Huai-Hai and northwestern AEZs) were much lower than those in the water-rich southern regions (e.g., AEZs in the southwest and Sichuan Basin). This is because the irrigation consumption in the north was much higher than in the south. Thus, it is suggested that the WP results can mislead policy decisions for water management, as some research has argued that products should be traded from regions with high WPs to regions with low WPs (Chapagain and Hoekstra, 2008; Dalin et al., 2014). If more wheat would be sourced from China's water-scarce northern regions, it would require more irrigation and place a huge amount of pressure on the local water sources. However, although the IWP indicator can illustrate the unsustainable water use of China's wheat production to a certain degree, this concept can also be confusing because it still fails to consider variations in the environmental relevance of water from different locations. Several previous studies have illustrated that water use indicators that do not consider environmental relevance have the potential to misinform and motivate behaviors that potentially conflict with the goal of reducing pressure on freshwater systems (Huang et al., 2014; Ridoutt and Huang, 2012; Ridoutt and Pfister, 2010a). This study, again, illustrated that high IWPs can also occur in water-stressed regions, resulting in very high environmental impacts (mango color in Fig. 4a).

By applying both IWP and WSF indicators, this study demonstrated that the current water use for wheat production in the water-scarce northern regions, where the IWPs were low but the WSFs were high, is highly unsustainable. The hotspot regions accounted for 34% of the total wheat cropping area. Considering all the regions with high WSFs, the contribution of hotspot regions was as high as 54% (marked red, light coral and mango colors in Fig. 4a). An important conclusion to be drawn from this study is that the pressure that wheat production puts on freshwater systems arises from the current patterns of water consumption, which often occurs in highly water-stressed regions. Wheat has a very wide suitable growing zone in China (IIASA/FAO, 2012). However, this study found that more than 60% of the total national wheat production was concentrated in the water-scarce Huang-Huai-Hai region, indicating that extensive wheat production in this region prohibited water sustainability.

Davis et al. (2017) identified that optimizing the global distribution of major crops can reduce the current consumptive use of blue water by 12% while increasing the production, and this was substantial compared with solutions such as improvements in crop WP and the minimization of food waste. In the case of China's wheat production, the priority for reducing this pressure can be given to optimizing the current water use patterns by redistributing the national wheat cropping. Historically, southern China was also an important contributor of wheat production. However, the wheat production in some southern regions including the AEZs in Jiangnan, Sichuan, the southwest and the south has decreased by 44% from 1980 to 2015 (NBSC, 1981–2016NBSC, 2016NBSC, 1981–2016). Due to numerous socioeconomic factors, especially the shifting of the labor force from rural to urban and suburban areas, more and more agricultural land with high quality lie fallow each winter in south China. A land area of 2.1×10^7 ha, which is suitable for winter wheat production, lie fallow in the middle-lower reaches of the Yangtze basin, accounting for 46% of the arable land in the region (Bao et al., 2014; Zhai et al., 2012). Thus, China's wheat production is experiencing a paradox—wheat is mainly produced in severely water-scarce regions while the suitable farmland in the water-rich regions lie fallow. To solve this problem, a national wheat cropping adjustment is necessary and urgent.

To overcome the mismatch of water availability and water consumption between the south and the north, China has been developing approximately 20 major water transfer projects, including the world's largest—the South-North Water Transfer Project (Liu et al., 2013). Furthermore, the Chinese government made a decision in 2011 to invest approximately 630 billion USD into water conservation from 2012 to 2020 and planned to establish a pricing mechanism to encourage saving water within a decade (Huang and Yang, 2017). On cultivated land, priority has been given towards improving land productivity through developing "high-standard farmlands" that are highly drought- and flood-resistant (Huang and Yang, 2017). All these strategies can alleviate the regional water stress to a certain degree. However, this study revealed that water consumption in some places has a greater potential for environmental harm than in others. It is the consumption patterns rather than the overall water consumption that deserves more attention in policy development. Fortunately, in 2016, the Chinese government announced a pilot plan called the Winter Fallow Policy in the Heilonggang region located in the Huang-Huai-Hai region, where the groundwater level has declined rapidly in recent years due to irrigation. By providing a certain number of subsidies called Ecological Compensations, farmers in the Heilonggang region were encouraged to abandon traditional wheat production. However, the Heilonggang region only accounted for a small part of the water-scarce region (less than 2% of the hotspot regions identified by this study). Thus, the Winter Fallow Policy has little impact on the regional water use. In addition, political decisions on land and water use lead to changes in the food supply system, which can have important environmental consequences extending beyond the local region (Huang et al., 2014). It

is therefore essential that strategies are aimed at sustainable water use to better integrate food security, the socioeconomic situation and the environment.

5. Conclusions

This study has highlighted the importance of putting regional freshwater issues into a national context. The water indicator results obtained in this study lead to several strategic implications for China's wheat production. First, efforts to address environmental impacts benefit from being guided by WSFs rather than other volumetric-based indicators. High WSF values highlight the need for more urgent actions. Second, the national adjustment of cropping has a high potential to alleviate regional water stress. Opportunities to increase wheat production in southern regions can be explored. Third, regional decisions could avoid unintended negative consequences by integrating national water, food and socioeconomic considerations. It is critical that policies affecting land and water use consider the wider implications of meeting national food demands. Moving beyond these strategic recommendations, further research with a narrower scope is recommended to assess the specific managerial options. This case study of China's wheat production is likely to be representative of the challenges faced by many of the world's countries, where pressures on land and water resources are high and a sustainable means of increasing food supply must be found.

Acknowledgments

This work was supported by China's National Key Research and Development Program (grant number 2016YFD0300210); and the Longshan Academic Talent Research Supporting Program of SWUST (grant numbers 18LZXT06 and 18LZX449). Jing Huang is grateful for the scholarship she received from the China Scholarship Council (grant number201808510050). We greatly thank Dr. Feng Huang and Dr. Qingquan Chu from CAU for their valuable comments on the manuscript.

Appendix A. Supplementary data

Supplementary material related to this article can be found, in the online version, at doi:https://doi.org/10.1016/j.agwat.2019.105744.

References

Aldaya, M.M., Chapagain, A.K., Hoekstra, A.Y., Mekonnen, M.M., 2012. The Water Footprint Assessment Manual: Setting the Global Standard. Taylor & Francis, Hoboken, New Jersey.

Bao, W., Liu, Y., Huang, Z., Wang, C., Zhou, L., Zhu, Z., Chen, L., Zhang, Y., Wu, B., Tong, H., 2014. Key technologies of developing wheat and barley production in winter fallow fields in middle and low reaches of Yangtze river. Hubei Agric. Sci. 53, 2729–2733 In Chinese).

Brown, L., 1997. Who will feed China? Wake-up call for a small planet. Int. J. Child. Rights 5, 504–506. https://doi.org/10.1163/15718189720493762.

Cai, J., Varis, O., Yin, H., 2017. China's water resources vulnerability: a spatio-temporal analysis during 2003–2013. J. Clean. Prod. 142, 2901–2910. https://doi.org/10.1016/j.jclepro.2016.10.180.

Cao, X., Wang, Y., Wu, P., Zhao, X., Wang, J., 2015. An evaluation of the water utilization and grain production of irrigated and rain-fed croplands in China. Sci. Total Environ. 529, 10–20. https://doi.org/10.1016/j.scitotenv.2015.05.050.

Cao, X.C., Wu, P.T., Wang, Y.B., Zhao, X.N., 2014. Assessing blue and green water utilisation in wheat production of China from the perspectives of water footprint and total water use. Hydrol. Earth Syst. Sci. 18, 3165–3178. https://doi.org/10.5194/hess-18-3165-2014.

Chapagain, A.K., Hoekstra, A.Y., 2008. The global component of freshwater demand and supply: an assessment of virtual water flows between nations as a result of trade in agricultural and industrial products. Water Int. 33, 19–32. https://doi.org/10.1080/02508060801927812.

CMWR (China Ministry of Water Resource), 2000-2015. Water Resource Bulletin Dataset 2000-2015. http://www.mwr.gov.cn/sj/tjgb/szygb/ (Accessed 10 October 2018).

Dalin, C., Hanasaki, N., Qiu, H., Mauzerall, D.L., Rodriguez-Iturbe, I., 2014. Water resources transfers through Chinese interprovincial and foreign food trade. Proc. Natl. Acad. Sci. U. S. A. 111, 9774–9779. https://doi.org/10.1073/pnas.1404749111.

Dalin, C., Qiu, H., Hanasaki, N., Mauzerall, D.L., Rodriguez-Iturbe, I., 2015. Balancing water resource conservation and food security in China. Proc. Natl. Acad. Sci. U. S. A. 112, 4588–4593. https://doi.org/10.1073/pnas.1504345112.

Davis, K.F., Rulli, M.C., Seveso, A., D'Odorico, P., 2017. Increased food production and reduced water use through optimized crop distribution. Nat. Geosci. 10, 919–924. https://doi.org/10.1038/s41561-017-0004-5.

Du, T., Kang, S., Zhang, J., Davies, W.J., 2015. Deficit irrigation and sustainable water-resource strategies in agriculture for China's food security. J. Exp. Bot. 66, 2253–2269. https://doi.org/10.1093/jxb/erv034.

Du, T., Kang, S., Zhang, X., Zhang, J., 2014. China's food security is threatened by the unsustainable use of water resources in North and Northwest China. Food Energy Secur. 3, 7–18. https://doi.org/10.1002/fes3.40.

Foley, J.A., Ramankutty, N., Brauman, K.A., Cassidy, E.S., Gerber, J.S., Johnston, M., Mueller, N.D., O'Connell, C., Ray, D.K., West, P.C., Balzer, C., Bennett, E.M., Carpenter, S.R., Hill, J., Monfreda, C., Polasky, S., Rockström, J., Sheehan, J., Siebert, S., Tilman, D., Zaks, D.P.M., 2011. Solutions for a cultivated planet. Nature 478, 337–342. https://doi.org/10.1038/nature10452.

Geng, Q., Ren, Q., Nolan, R.H., Wu, P., Yu, Q., 2019. Assessing China's agricultural water use efficiency in a green-blue water perspective: a study based on data envelopment analysis. Ecol. Indic. 96, 329–335. https://doi.org/10.1016/j.ecolind.2018.09.011.

Heilig, G.K., Fischer, G., Van Velthuizen, H., 2009. Can China feed itself? An analysis of China's food prospects with special reference to water resources. Int. J. Sustain. Dev. World Ecol. 7, 37–41. https://doi.org/10.1080/13504500009470038.

Huang, J., Scherer, L., Lan, K., Chen, F., Thorp, K.R., 2019. Advancing the application of a model-independent open-source geospatial tool for large spatiotemporal simulations. Environ. Model. Softw. 119, 374–378. https://doi.org/10.1016/j.envsoft.2019.07.003.

Huang, F., Li, B., 2010. Assessing grain crop water productivity of China using a hydro-model-coupled-statistics approach. Part II: application in breadbasket basins of China. Agric. Water Manag. 97, 1259–1268. https://doi.org/10.1016/j.agwat.2010.02.017.

Huang, J., Ridoutt, B.G., Zhang, H., Xu, C., Chen, F., 2014. Water footprint of cereals and vegetables for the Beijing market: comparison between local and imported supplies. J. Ind. Ecol. 18, 40–48. https://doi.org/10.1111/jiec.12037.

Huang, J., Yang, G., 2017. Understanding recent challenges and new food policy in China. Glob. Food Secur. 12, 119–126. https://doi.org/10.1016/j.gfs.2016.10.002.

IIASA/FAO, 2012. Global Agro-ecological Zones (GAEZ v3.0). IIASA/FAO, Rome, Italy.

Kang, S., Hao, X., Du, T., Tong, L., Su, X., Lu, H., Li, X., Huo, Z., Li, S., Ding, R., 2017. Improving agricultural water productivity to ensure food security in China under changing environment: from research to practice. Agric. Water Manag. 179, 5–17. https://doi.org/10.1016/j.agwat.2016.05.007.

Khan, S., Hanjra, M.A., Mu, J., 2009. Water management and crop production for food security in China: a review. Agric. Water Manag. 96, 349–360. https://doi.org/10.1016/j.agwat.2008.09.022.

Liu, X.H., Chen, F., 2005. Farming Systems in China. China Agriculture Press, Beijing, China (In Chinese).

Liu, J., Wiberg, D., Zehnder, A.J.B., Yang, H., 2007a. Modeling the role of irrigation in winter wheat yield, crop water productivity, and production in China. Irrig. Sci. 26, 21–33. https://doi.org/10.1007/s00271-007-0069-9.

Liu, J., Williams, J.R., Zehnder, A.J.B., Yang, H., 2007b. GEPIC - modelling wheat yield and crop water productivity with high resolution on a global scale. Agric. Syst. 94, 478–493. https://doi.org/10.1016/j.agsy.2006.11.019.

Liu, J., Zang, C., Tian, S., Liu, J., Yang, H., Jia, S., You, L., Liu, B., Zhang, M., 2013. Water conservancy projects in China: achievements, challenges and way forward. Glob. Environ. Change 23, 633–643. https://doi.org/10.1016/j.gloenvcha.2013.02.002.

Mekonnen, M.M., Hoekstra, A.Y., 2010. A global and high-resolution assessment of the green, blue and grey water footprint of wheat. Hydrol. Earth Syst. Sci. 14, 1259–1276. https://doi.org/10.5194/hess-14-1259-2010.

NBSC (National Bureau of Statistics of China). China Statistical Yearbook 1981-2016. http://www.stats.gov.cn/tjsj/ndsj/ (Accessed 20 October 2018).

Pfister, S., Bayer, P., 2014. Monthly water stress: spatially and temporally explicit consumptive water footprint of global crop production. J. Clean. Prod. 73, 52–62. https://doi.org/10.1016/j.jclepro.2013.11.031.

Pfister, S., Koehler, A., Hellweg, S., 2009. Assessing the environmental impact of freshwater consumption in LCA. Environ. Sci. Technol. 43, 4098–4104. https://doi.org/10.1021/es802423e.

Raes, D., Steduto, P., Hsiao, T.C., Fereres, E., 2009. Aquacrop—the FAO crop model to simulate yield response to water: II. Main algorithms and software description. Agron. J. 101, 438–447. https://doi.org/10.2134/agronj2008.0140s.

Ridoutt, B.G., Huang, J., 2012. Environmental relevance—the key to understanding water footprints. Proc. Natl. Acad. Sci. U. S. A. 109, E1424. https://doi.org/10.1073/pnas.1203809109.

Ridoutt, B.G., Pfister, S., 2010a. A revised approach to water footprinting to make transparent the impacts of consumption and production on global freshwater scarcity. Glob. Environ. Change 20, 113–120. https://doi.org/10.1016/j.gloenvcha.2009.08.003.

Ridoutt, B.G., Pfister, S., 2010b. Reducing humanity's water footprint. Environ. Sci. Technol. 44, 6019–6021. https://doi.org/10.1021/es101907z.

Scherer, L., Pfister, S., 2016. Dealing with uncertainty in water scarcity footprints. Environ. Res. Lett. 11, 1–9. https://doi.org/10.1088/1748-9326/11/5/054008.

Scherer, L.A., Verburg, P.H., Schulp, C.J.E., 2018. Opportunities for sustainable intensification in European agriculture. Glob. Environ. Change 48, 43–55. https://doi.org/10.1016/j.gloenvcha.2017.11.009.

Siebert, S., Döll, P., 2010. Quantifying blue and green virtual water contents in global crop production as well as potential production losses without irrigation. J. Hydrol. 384, 198–217. https://doi.org/10.1016/j.jhydrol.2009.07.031.

Steduto, P., Hsiao, T.C., Raes, D., Fcreres, E., 2009. AquaCrop—the FAO crop model to

simulate yield response to water: I. Concepts and underlying principles. Agron. J. 101, 426–437. https://doi.org/10.2134/agronj2008.0139s.

Sun, S.K., Wu, P.Te, Wang, Y.B., Zhao, X.N., 2013. The virtual water content of major grain crops and virtual water flows between regions in China. J. Sci. Food Agric. 93, 1427–1437. https://doi.org/10.1002/jsfa.5911.

Thorp, K.R., Bronson, K.F., 2013. A model-independent open-source geospatial tool for managing point-based environmental model simulations at multiple spatial locations. Environ. Model. Softw. 50, 25–36. https://doi.org/10.1016/j.envsoft.2013.09.002.

Wieder, W.R., Boehnert, J., Bonan, G.B., Langseth, M., 2014. Regridded Harmonized World Soil Database v1.2. ORNL DAAC, Oak Ridge, Tennessee, USA. https://doi.org/10.3334/ORNLDAAC/1247.

Xiong, W., Conway, D., Lin, E., Xu, Y., Ju, H., Jiang, J., Holman, I., Li, Y., 2009. Future cereal production in China: the interaction of climate change, water availability and socio-economic scenarios. Glob. Environ. Change 19, 34–44. https://doi.org/10.1016/j.gloenvcha.2008.10.006.

Yang, H., Zhang, X., Zehnder, A.J.B., 2003. Water scarcity, pricing mechanism and institutional reform in northern China irrigated agriculture. Agric. Water Manag. 61, 143–161. https://doi.org/10.1016/S0378-3774(02)00164-6.

Zhai, M., Xu, X., Jiang, X., 2012. A method on information extraction on winter fallow fields in middle and lower reaches of Yangtze River by remote sensing. J. Geo-Inf. Sci. 14, 389–397 (In Chinese).

Zhang, F.C., Liu, X.G., Yang, Q.L., 2015. Theory and Practice on High Efficient Use of Water and Fertilizer by Crop in Arid Region of Northwest of China. China Science Press, Beijing, China (In Chinese).

Zhuo, L., Mekonnen, M.M., Hoekstra, A.Y., 2016. The effect of inter-annual variability of consumption, production, trade and climate on crop-related green and blue water footprints and inter-regional virtual water trade: a study for China (1978–2008). Water Res. 94, 73–85. https://doi.org/10.1016/j.watres.2016.02.037.

Zuo, L., Zhang, Z., Carlson, K.M., MacDonald, G.K., Brauman, K.A., Liu, Y., Zhang, W., Zhang, H., Wu, W., Zhao, X., Wang, X., Liu, B., Yi, L., Wen, Q., Liu, F., Xu, J., Hu, S., Sun, F., Gerber, J.S., West, P.C., 2018. Progress towards sustainable intensification in China challenged by land-use change. Nat. Sustain. 1, 304–313. https://doi.org/10.1038/s41893-018-0076-2.